Laser Surface Texturing of AA1050 Aluminum Alloy: Optimization of Geometric Patterns and Laser Parameters for Enhanced Surface Characteristics

Satılmış ÜRGÜN [a] , Sinan FİDAN [b], Mustafa Özgür BORA [c], Demet ÜRGÜN [d], Çağla PİLAVCI [e,f], Timur CANEL [g]

[a] Kocaeli University, Faculty of Aeronautics and Astronautics, Department of Aviation Electrics and Electronics, Kocaeli, Turkey, urgun@kocaeli.edu.tr

[b] Kocaeli University, Faculty of Aeronautics and Astronautics, Department of Airframe & Powerplant Maintenance, Kocaeli, Turkey, sfidan@kocaeli.edu.tr

[c] Kocaeli University, Faculty of Aeronautics and Astronautics, Department of Airframe & Powerplant Maintenance, Kocaeli, Turkey ozgur.bora@kocaeli.edu.tr

[d] Kocaeli University, Kocaeli, Turkey demettaskan90@gmail.com

[e] Department of Physics, Kocaeli University, Kocaeli, Turkey, cagla.pilavci@gmail.com

[f] TUBITAK Marmara Research Center Life Sciences, Kocaeli, Turkey, cagla.pilavci@gmail.com

[g] Department of Physics, Kocaeli University, Kocaeli, Turkey, tcanel@kocaeli.edu.tr

Abstract

This study investigates the optimization of laser surface texturing (LST) parameters on AA1050 aluminum alloy using fiber laser technology. Four geometric patterns—square, diamond, hexagon, and circle—were tested under varying laser power (40-100 W) and theoretical scanned area factors (20-80%). Surface roughness was characterized using a profilometer, and the morphology was analyzed with an optical microscope. Results indicated that at the lower laser power and higher factors of the scanned area, surface roughness was increased, while at higher power, it decreased owing to the smoothing effect. The most promising results were obtained for a square pattern at a 40 W laser power and an 80% area factor, showing clear texturing with increased roughness. Angle of contact measurements showed improved wettability for certain laser parameter combinations. The obtained results have indicated that adequate control of the LST parameters can bring about improvement in functional properties for industrial applications in the AA1050 surface.

Keywords: Laser Surface Texturing (LST), AA1050 alloy, Roughness, Laser Parameter Optimization, Contact angle.

Çağla PİLAVCI: 0009-0005-5237-9598
Satılmış ÜRGÜN: 0000-0003-3889-6909
Timur CANEL: 0000-0002-4282-1806
Sinan FİDAN: 0000-0003-4385-4981

Özet

Bu çalışma, AA1050 alüminyum alaşımı üzerinde fiber lazer teknolojisi kullanarak lazer yüzey dokulama (LST) parametrelerinin optimizasyonunu incelemektedir. Kare, elmas, altıgen ve daire olmak üzere dört geometrik desen, değişken lazer gücü (40-100 W) ve teorik taranan alan faktörleri (20-80%) altında test edilmiştir. Yüzey pürüzlülüğü bir profilometre ile karakterize edilmiş ve morfoloji optik mikroskop ile analiz edilmiştir. Sonuçlar, düşük lazer gücünde ve yüksek taranan alan faktörlerinde yüzey pürüzlülüğünün arttığını, ancak daha yüksek güçte, yüzeyin düzgünleşmesi nedeniyle azaldığını göstermiştir. En umut verici sonuçlar, 40 W lazer gücünde ve %80 alan faktöründe kare deseni için elde edilmiş olup, belirgin dokulama ve artan pürüzlülük göstermiştir. Temas açısı ölçümleri, belirli lazer parametre kombinasyonları için ıslanabilirlikte iyileşme olduğunu göstermiştir. Elde edilen sonuçlar, LST parametrelerinin uygun bir şekilde kontrol edilmesiyle, AA1050 yüzeyi için endüstriyel uygulamalarda işlevsel özelliklerin iyileştirilebileceğini göstermiştir.

Anahtar Kelimeler: Lazer Yüzey Dokulandırma (LST), AA1050 alaşımı, Pürüzlülük, Lazer Parametresi Optimizasyonu, Temas Açısı.

1. Introduction

A permanently rising demand for light solutions in general, and especially in transportation, is a challenge for modern industry. It is due to these favourable properties that light materials like aluminum, magnesium, and titanium alloys have been gaining more and more popularity. Among them, aluminum alloys play the leading role, since they effectively combine good corrosion resistance with a high strength-to-weight ratio. With these qualities, the aluminum alloys have found applications in engineering of many kinds-for example, in packaging and the automotive industry-where toughness and performance are often called for [1]. In general, several surface modification methods, such as mechanical processing, chemical etching, electrochemical treatment, and laser texturing, have been developed to provide optimized surface roughness by anodizing. However, a number of these technologies have practical realization that is problematic due to long processing times, high costs, or difficulty in handing non-flat components and complex geometries. In addition, techniques may influence the material's corrosion resistance, durability, and mechanical properties, and thus adequate optimization is called for between surface alteration and material integrity. [2]. Commercially pure (CP) aluminum can be surface functionalized in some applications to improve wear and friction resistance, especially in the aerospace and automotive industries. In some situations, as in printing plate applications, functionalization is utilised to impart new surface qualities, like topographies and wettability to water and oils. Due to its many benefits, such as being highly automatable, delivering outstanding repeatability and accuracy, being environmentally friendly, and offering a moderately priced solution, laser surface texturing has become an especially useful approach. These characteristics make laser texturing a desirable choice for accurate and long-lasting surface alteration [3].

Boinovich et al. [4] showed that surface texturing for producing multimodal roughness, one of the deciding processes in the preparation of superhydrophobic coatings, may simultaneously change the physicochemical properties of the substrate surface layer. By variation of the laser treatment conditions, various coatings with different oxide layer barriers have been produced. Results show that the aluminum alloy is heated locally and rapidly after intensive laser treatment due to the interaction of a high-power nanosecond laser beam. As a result of this process, an oxide surface layer with improved barrier qualities is formed, which effectively prevents charges, chloride ions, and water molecules from transferring. The evaluation of the adherence of electroplated nickel and electroless NiP coatings, varying in thickness from 5 to 20 μm, on aluminum substrates with different surface qualities has been conducted [5]. The substrate coupons were prepared using a variety of methods, including sandblasting, grinding, polishing, and laser surface texturing, to provide a variety of textures and levels of roughness. The combination of sandblasting and laser texturing resulted in a more hydrophilic surface than each treatment alone and enhanced coating adherence. The important factors for adhesion behavior of specimens are surface skewness (Rsk) and surface texture anisotropy (Str). A nanoporous anodic oxide layer was formed on aluminum by self-organized anodization in sulfuric acid after laser pre-treatment. Using quantitative analyses of FE-SEM images, the effects of laser pre-treatment parameters and the directly solidified aluminum grain size on

the formation of the nanoporous anodic aluminum oxide (AAO) were examined. These results indicated that key parameters such as pore diameter, interpore spacing, and the thickness of the anodic oxide layer formed were independent of the laser pre-treatment. This result tends to imply that the basic structural properties of the anodic oxide layer do not change with laser pretreatment [6]. The theory of laser ablation is discussed [7], along with how it affects the physicochemical characteristics of metallic materials and how it affects adhesive-bonded parts' corrosion resistance and bonding strength. Min et al. [7] examine the principles that underlie the improved bonding performance of joints made from metallic surfaces ablated with a laser. In other words, the bonding strength of adhesively bonded joints, previously treated by laser ablation, increases due to improvement in both wettability and surface roughness of the metallic adherend. This was possible only if the adhesive can sufficiently wet the laser-ablated surface to develop the mechanical interlocking at the bonding surfaces. Therefore, to maximize joint function, surface texture and adhesive compatibility are both essential. The absorptance measurements on engineering-grade nonferrous metals, such as aluminum (Al), copper (Cu), and zinc (Zn) alloys, performed at room temperature are reported [8]. No apparent dependency between absorptance and surface roughness could be observed on low levels of roughness (Sa 0.15–0.60), but for a separate batch of rougher samples, a high correlation of roughness to absorptance (Sa 2.34) was found, suggesting that at a higher level of roughness, surface texture might affect absorptance. Siddiqui et al. [9] have explored the metallurgical and mechanical properties of LSA-treated AlxCu0.5FeNiTi HEA on aluminum alloy (AA1050). In turn, the enhanced microhardness and composite structure created by the HEA layer are recognized as the key factors for the erosion rate reduction of the LSA-treated substrate in the mentioned study. Such enhancements in surface characteristics lead to increased wear resistance and durability of the treated alloy.

This study aimed at optimizing geometric patterns and laser parameters in surface texturing of an aluminum alloy AA1050 with the purpose of enhancing properties on the surface. The variation of power of laser, type of texture, theoretical laser scanned area factor (%), and other laser properties is done systematically by researchers to find out how different laser parameters affected the surface modification. Because of the precision and effectiveness of fiber laser technology at surface structuring, it is used for generating customized surface textures. Surface topography and roughness after the laser treatments were characterized by 3D optical profilometer analysis, while the changes in wettability were quantified by contact angle measurements from the textured surfaces. These also helped improve the performance of later engineering applications by showing how different parameters of the laser influence the functional surface characteristics of the aluminum alloy.

2. Experimental Procedures

2.1 Material

The material used in this study is the AA1050 aluminum alloy, characterized by very high purity and excellent mechanical properties. The basic chemical composition of AA 1050 includes at least 99.5% of aluminium and the rest are the conglomeration elements, namely, silicon (Si) up to 0.25%, iron (Fe) up to 0.4%, copper (Cu) up to 0.05%, manganese (Mn) up to 0.05%, magnesium (Mg) up to 0.05%, zinc (Zn) up to 0.1%, and titanium (Ti) up to 0.05%. This alloy also pertains to other elements, each individually limited to a maximum of 0.05% with a total of 0.15%. At the mechanical properties level, the AA1050 alloy has a tensile strength between 90 to 165 MPa and yield strength of 34 to 152 MPa depending on the conditions of processing. The material also features reasonable ductility: the elongation percentage varies between 2% and 30%. These characteristics make AA1050 aluminum alloy a versatile material in general industry for applications requiring high corrosion resistance, excellent formability, and good conductivity.

2.2 Laser Surface Texturing Process

This work presents the engraving of various geometrical patterns onto the surface of an AA1050 series aluminium alloy by Fiber laser technology (Figure 1). Four geometric patterns were tested, namely: Square, Diamond, Hexagon, and Circle. Each of these patterns was subjected to four different "Theoretical laser scanned area factors (%)": 80%, 60%, 40%, and 20%. Similarly, four other different laser power levels have been considered, namely: 40 W, 60 W, 80 W, and 100 W. These experiments were conducted to understand how the surface roughness, microstructure properties, and surface energy of laser-processed surfaces respond to changing laser parameters and surface geometries. The textures were characterized based on the shape of the laser-applied patterns, and for each geometric pattern, several experimental conditions were tested. The aim of this work is to investigate the effects of laser processing parameters on the surfaces of aluminum and to establish the conditions under which optimum surface properties can be achieved.

Fibre lasers are efficient and reliable systems capable of producing high-intensity laser beams. They are widely used in materials processing, micromechanical applications and marking processes. Highlights of fibre lasers include low maintenance, high beam quality, energy efficiency and long lifetime. A fibre laser with a power output of 100W is ideal for applications requiring medium to high power and is generally effective for cutting, marking and surface modification of metals.
In the system shown in the figure, a computer provides full control and programming of the laser. The control unit of the laser controls the power of the laser output, pulse duration, and other parameters. The fiber laser in this system generates a high-intensity output laser light which is transmitted through optical fibers to the laser scanning head. The laser scanning head scans the laser beam fast and precisely on the sample by galvanometer mirrors. Theta lens optimizes the profile of the beam by deflecting the laser beam onto a specific point. During this process, the sample is subjected to the laser beam, where, in this example, it is 1050 series aluminium. The height can be adjusted in this platform where the sample is subjected to optimize the distance between the laser beam and the sample. The system is especially well-suited for undergoing processes such as laser texturing, engravings and surface treatment and can process soft metals like 1050 series aluminium effectively.

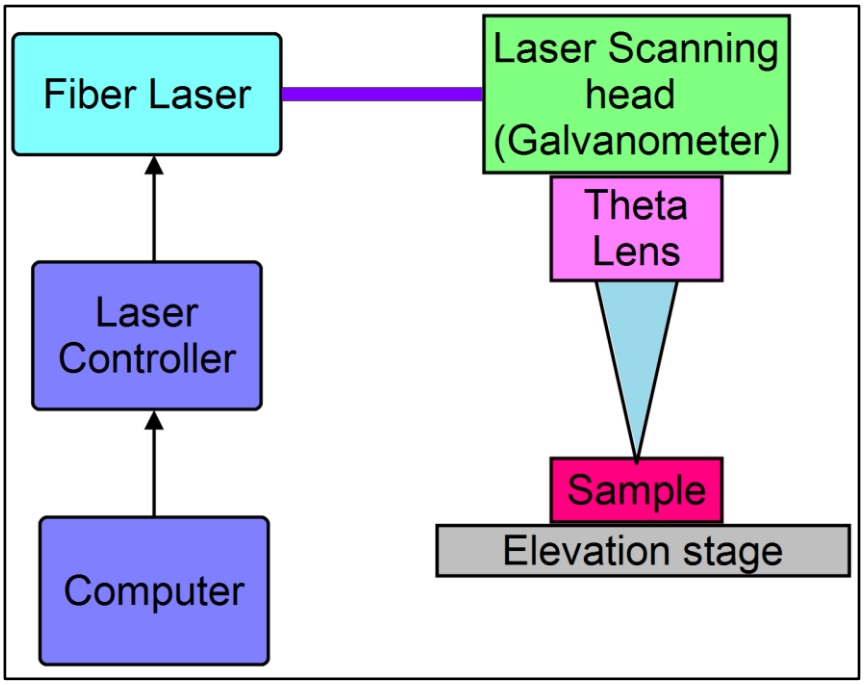

Figure 1. *Laser surface texturing schematic of AA1050 alloy.*

2.3 Roughness Characterization

The morphology of the AA1050 alloy surfaces after surface texturing by laser was acquired by non-contact laser profilometry. For that, a profilometer, known as the Nanovea PS50, was employed. This equipment enables the direct visualization without contact of a fraction of the characteristics presented by the superficial roughness. After that, raw profilometer data of the samples were analyzed by applying Digital Surf edition, version 6.2.7487, from Mountains Technology. This software facilitated the creation of three-dimensional surface topography representations in accordance with ISO 25178 standards. Additionally, the key images necessary for determining the laser-induced surface topographies were generated in line with ISO 4287 standards. The laser profilometer enabled a comprehensive examination of the entire LST surface by scanning the sample surfaces, particularly those treated with the various laser parameters, over an area of 3 mm by 3 mm. The analysis was performed on samples subjected to different textures, theoretical laser scanned area factors, and power levels, as outlined in the table, to accurately characterise the resulting surface modifications on the AA1050 alloy.

2.4 Optical Microscope Surface Characterization

Characterization at the surface of the AA1050 aluminum alloy used in this study was done by using an Evident-Olympus BX 53MRF model microscope. This optical microscope provided high-resolution microstructures that were detailed images of the exact microstructural features forming on laser-textured surfaces. The BX 53MRF model possesses several magnifications provided, by which surface morphology could be precisely examined without any enlargement and the micro-defects created by laser processing identified, including grain structures and surface roughness. Characterization was a fundamental process that gave detailed information on how various laser parameters affected the surface quality and microstructure of the AA1050 alloy, thus helping in further understanding these factors for influencing specific performance of the material in practical applications.

2.5 Contact Angle Measurements

To examine the effects of surface texture parameters on the contact angle in detail, 4 different patterns were formed in an area of 2.5x2.5 cm2. Contact angle measurements were made using the KSV optical contact angle and surface tension meter. Contact angle measurements were made by dropping a very small drop of pure water on the laser-treated surfaces. The contact angle was measured two seconds after the water drop hit the surface. It was assumed that the collision effect was minimized in the second after the water drop hit the surface.

3. Results and Discussions

3.1. Roughness Characterization

In surface roughness assessment, Sa (arithmetical mean height) quantifies the average height variations of the surface topography and will be utilized to determine the roughness of the laser-treated surfaces. Surfaces with elevated Sa values exhibit greater surface roughness, whereas decreased Sa values indicate flatter and smoother surfaces. On the surface machined with an 80% theoretical laser scanning area factor and 40W laser power, as shown in Figure 2-a, clear square patterns could be seen. The Sa value on this surface is relatively high due to the distinctness of the patterns, which creates a distinct roughness on the surface. This roughness was caused by the scanning area's height and the laser's low power. In Figure 2-b, it is expected that the Sa value will be slightly lower on the square-patterned surface machined with 60% theoretical laser scanning area factor and 60W laser power. It is observed that the surface patterns remain distinct, but the increase in laser power reduces the surface roughness. Figure 2-c: for the square textured surface processed with 40% theoretical laser scanning area factor and 80W laser power, the Sa value will be even lower due to the flatter surface. High laser power caused the surface's details to decrease, resulting in a reduction in roughness. Figure 2-d illustrates that when processing a square textured surface with a 20% theoretical laser scanning area factor and 100W laser power, the Sa value is relatively low. The smoothness of the surface indicates that the laser almost melted the surface, and it lost its texture wholly. Figure 2-e represents a diamond-textured surface treated by 80% theoretical laser scanning area factor and by 60 W laser power. There is a high value of Sa due to clarity in the patterns and the roughness of the surface. This value shows that the surface retains regular and obvious textured structures. The Sa-value is slightly lower in the case of a 60% theoretic laser scanning area factor and laser power input of 40 W applied on the diamond-textured surface shown in Fig. 2-f. However, the surface still displays clear patterns. This translates to a smoother topography with minimal surface deformation. Figure 2-g shows a lower Sa value on the diamond-patterned surface, which was processed using a 40% theoretical laser scanning area factor and 100W laser power. High laser power caused the surface to be smoother and the patterns to lose their clarity. Figure 2-h shows a relatively low Sa value on the diamond-patterned surface, which was processed using a 20% theoretical laser scanning area factor and 80W laser power. The surface texture is almost completely flattened, and the roughness is minimized. Figure 2-i shows that the hexagonal patterned surface, processed with an 80% theoretical laser scanning area factor and 80W laser power, has a high Sa value. The roughness and clarity of the surface patterns cause this. Figure 2-j shows a slightly lower Sa value on the hexagonal patterned surface, which was processed using a 60% theoretical laser scanning area factor and 100W laser power. High laser power caused the edges of the patterns to become softer and the roughness to decrease. Fig. 2-k, the hexagonal patterned surface processed with 40% theoretical laser scanning area factor and 40W laser power, contains a high amount of Sa. It is observed that the surface contains a well-defined and deep pattern which shows its extreme roughness. Fig. 2-l presents hexagonal patterned surface processed with 20% theoretical laser scanning area factor and 60W laser power having lower value of Sa. The surface roughness is reduced because it is softer and less rough. In Figure 2-m, the circle-patterned surface, processed with an 80% theoretical laser scanning area factor and 100W laser power, exhibits a high Sa value. The circle patterns on the surface are distinct and contribute to the high roughness. It is predicted a

medium value of Sa for the circle-patterned surface processed by 60% theoretical laser scanning area factor with 80W laser power in Figure 2-n. This is since the sharpness of patterns in the surface is balanced by the overall roughness. Figure 2-o shows a high Sa value on the circular patterned surface, which was processed using a 40% theoretical laser scanning area factor and 60W laser power. The clarity and roughness of the surface patterns are high. Figure 2-p shows a low Sa value on the circular patterned surface, which was processed using a 20% theoretical laser scanning area factor and 40W laser power. The flatter surface and less distinct patterns reduce roughness. As a result, Sa values reflect the effect of laser parameters on surface textures; higher laser power and lower scanning area factors generally lead to lower roughness (Sa), while lower power and higher scanning area factors result in higher Sa values.

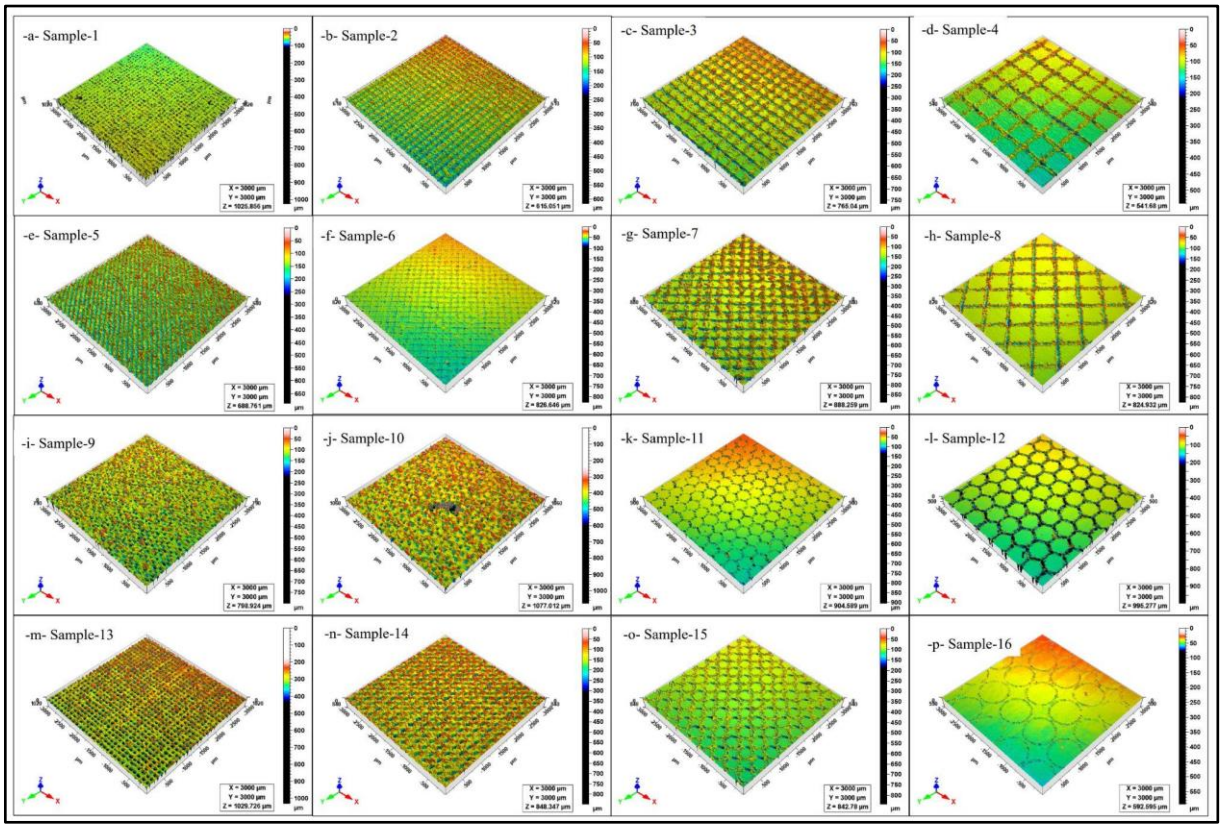

Figure 2. *Laser surface textured AA1050 alloy surface 3D profilometer images.*

3.2. Surface Optical Microscope Characterization

Figure 3-a shows the surface of an AA1050 aluminum alloy processed with a square texture. In this sample, laser processing was performed using 80% theoretical laser scanning area factor and 40W laser power. In the image, it is evident that the square patterns are quite clear and have sharp edges. The relatively low laser power prevented overheating on the surface and preserved the pattern's clarity. Figure 3-b depicts another sample with a square texture. This sample was processed with 60% theoretical laser scanning area factor and 60W laser power. The patterns are still recognizable and clear, but a slight softening is observed at the edges. This situation shows that the increase in laser power causes more thermal effects on the surface. Figure 3-c represents a square textured surface processed using 40% theoretical laser scanning area factor and 80W laser power. The patterns are still observable but less distinct compared to the previous samples. The higher laser power caused more material movement on the surface and less clear edges. Figure 3-d shows a square textured surface processed with a 20% theoretical laser scan area factor and 100W laser power. In this sample, patterns are quite difficult to recognize, and significant material deformation is observed on the surface. High power and low scan area factors caused excessive heating and melting on the surface, which negatively affected the clarity of the patterns. Figure 3-e represents a surface treated with diamond texture. This sample was created using an 80% theoretical laser scan area factor and 60W laser power. The patterns are clearly defined and well visible on the surface. Moderate laser power ensured that the pattern was preserved without excessive deformation on the surface. Figure 3-f shows a surface processed again with diamond texture. In this sample, a 60% theoretical laser scan area factor and 40W

laser power were used. The patterns are clearly defined, and the edges appear sharper. Low power increased the pattern's clarity while having minimal thermal effects on the surface. Figure 3-g shows a surface with a diamond pattern processed using 100W laser power with a 40% theoretical laser scanning area factor. The patterns on the surface are less distinct, and the edges are softened. High laser power causes more material shear on the surface and pattern distortion. Figure 3-h shows a surface with diamond texture processed using 80W laser power with a 20% theoretical laser scanning area factor. In this sample, the patterns are quite blurry, and significant deformation is observed on the surface. This demonstrates that a low scanning area factor and high laser power have undesirable thermal effects on the surface. Figure 3-i depicts a surface with a processed hexagonal texture. In this sample presently used, 80% theoretical laser scanning area factor and 80W laser power have been used or implemented. The overall patterns are appearing well; however, after high laser power, there has been a slight softening on the edges. Figure 3-j shows a surface with hexagonal texture treated using 100W laser power with a 60% theoretical laser scanning area factor. Features are observable but edges rounder and less clear. Higher power has stronger thermal effects in the surface. Figure 3-k: surface treated with hexagonal pattern, 40% theoretical laser scanning area factor, with a 40W laser power. Due to the low power of the laser, features are relatively clear and minor thermal effects can be obtained on the surface. This setting did a fine balance in terms of the preservation of the patterns. In Figure 3-l, a surface with a hexagonal texture processed using a laser power of 60W with theoretical laser scan area factor of 20%: the patterns are fuzzy and there are traces of melting on the surface. We can see that the low scan area factor and moderately powerful laser have issued unwanted deforming on the surface. In Fig. S1-m, surface with circular texture processed by laser power of 100W and theoretical laser scan area factor of 80%: it is possible to clearly distinguish the patterns, but the edges are a bit softened by the high laser power. In Fig. 3-n, surface with circular texture processed by laser power of 80W and theoretical laser scan area factor of 60%. The patterns are clear, the edges are well defined, and with minimal thermal deformation on the surface. These parameters provide a suitable balance for preserving the circular patterns. In Figure 3-o, a surface with a circular texture processed using a laser power of 60W with a theoretical laser scan area factor of 40%. The patterns have sharp and well-defined edges. A small magnitude of laser power is improving the visibility of the pattern. Figure 3-p is the surface that was processed at 40W laser power, with a circular texture, and a theoretical laser scan area factor of 20%. Patterns are blurry, while regarding the surface, one can appreciate a high deformation. The low scan area factor, together with the laser power, had a decisive negative impact on the pattern identifiability.

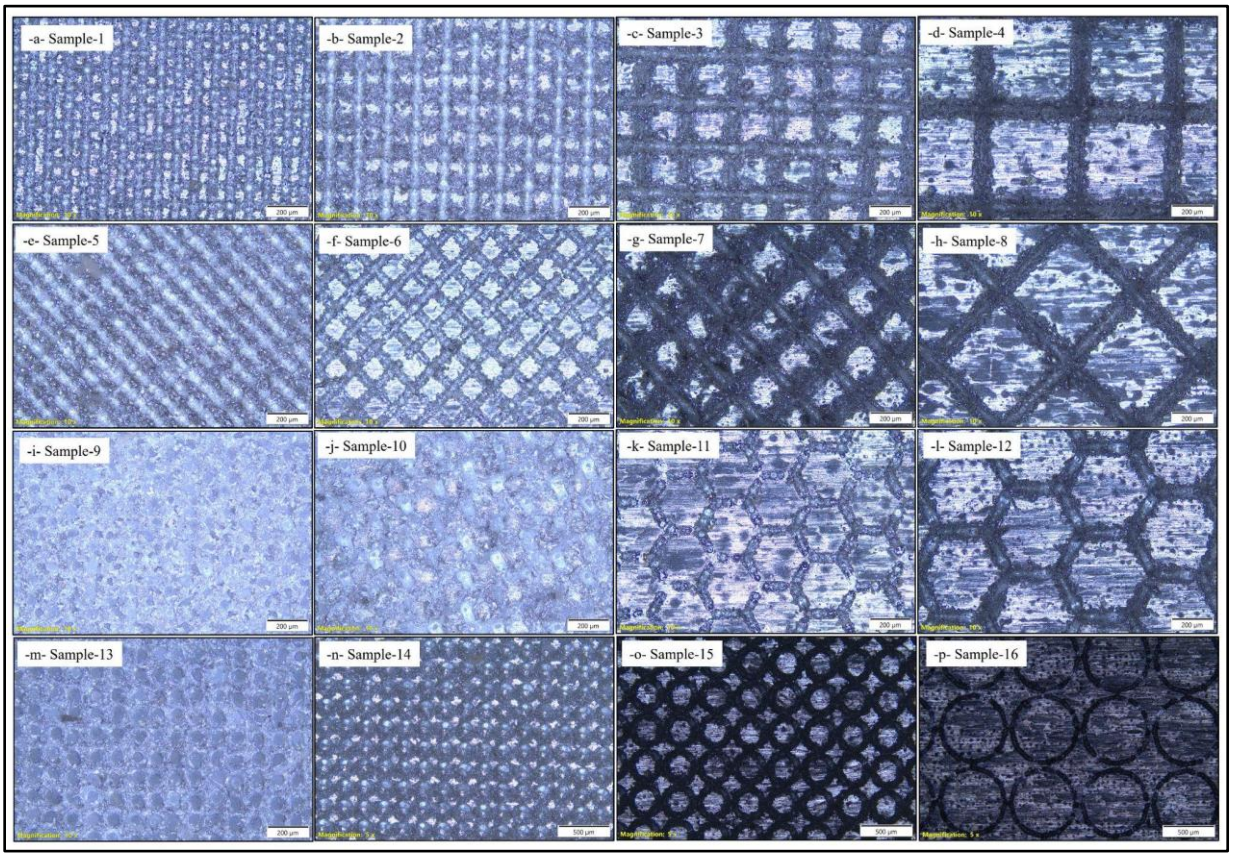

Figure 3. *Laser surface textured AA1050 alloy surface optical microscope images.*

3.3. Contact Angle Measurement and Characterization

In contact angle measurements, contact angle measurements of laser-textured surfaces were made. Since the contact angle for a hydrophobic surface should be the largest value, the 'larger the better' characteristic was used in Taguchi analysis. Accordingly, the best result, the highest contact angle, was obtained in experiment 15 with 159.49° as shown in Figure 4-a. As a result of experiments 10 and 11, the dripped liquid immediately dispersed on the surface, and measurements could not be taken. These two experiments may be the result of hydrophilicity, or they may be the result of an inhomogeneous surface. Because of this uncertainty, these results were ignored, and the parameters of these experiments are intended to be investigated in further studies. If these two experimental results are ignored, the worst result is obtained by experiment number 16 with 106.94° as shown in Figure 4-b. According to Table 1's ANOVA table and the Taguchi method, the parameter values that should be used to obtain the best result should be 'circle' for texture type, 80% for laser-scanned area factor, and 60 W for laser power. The experiment, conducted with the recommended parameter values, is predicted to yield a contact angle value of 159.90°. This value is better than the results obtained with 16 experiments.

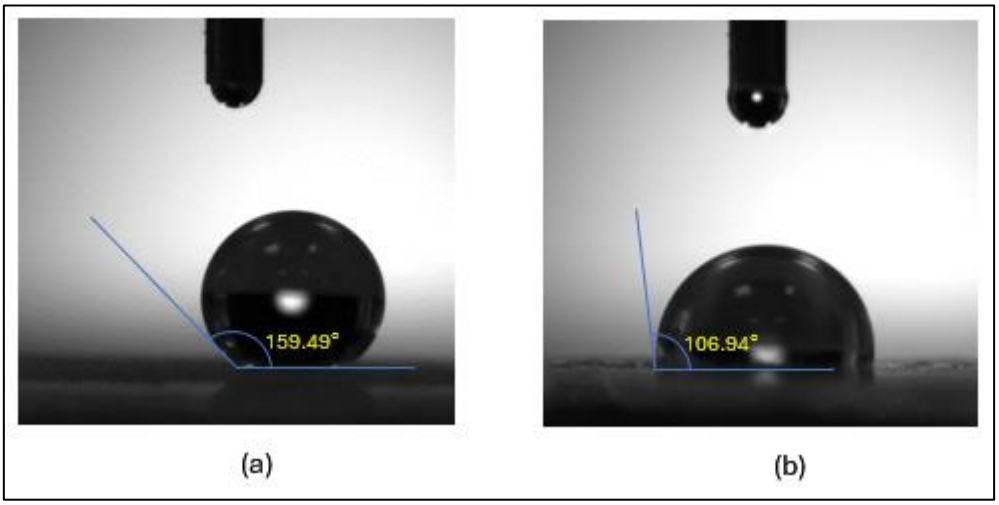

Figure 4. (a) The highest contact angle obtained with circle texture, 40 % scanned area factor, 60 W power, (b) the lowest contact angle obtained with circle texture, 20 % scanned area factor, 40 W power.

As shown in Table 1, the most effective parameter was calculated as laser power, with a value of 64.97%, because of ANOVA analysis. The second most effective parameter was the scanned factor, with a value of 34.54%. The least effective parameter was texture type with a value of 0.49%. Table 1 presents the experimental sets arranged according to the Taguchi L16 orthogonal array and an ANOVA table calculated based on the larger, better characteristics.

Table 1. ANOVA table according to Taguchi's "larger the better characteristics".

			Average S/N								
Factors	Unit	1st level	2nd level	3rd level	4th level	A	B	C	D	E	F
Texture		43.08	43.00	43.10	43.13	3	0.03	0.01	0.49	4	4
Scanned Factor	%	43.50	43.39	42.92	42.53	3	2.39	0.60	34.54	1	80%
Power	W	42.39	43.60	42.70	43.56	3	4.49	1.12	64.97	2	60 W
			43.07								
	Total						6.91		100.00		
	Optimum S/N										44.08
	Contact Angle (Degree)										159.90

The result of Analysis of variances for SN ratio and means were given in Table 2 and Table 3 respectively.

Table 3. Analysis of Variance for SN ratios

Source	DF	Seq SS	Adj SS	Adj MS	F	P
Texture Type	3	0.03	0.032	0.01	0.01	0.999
Scanned Factor	3	2.28	3.15	1.05	0.79	0.558
Laser Power	3	4.66	4.65	1.55	1.17	0.425
Residual Error	4	5.30	5.30	1.33		
Total	13	12.27				

Table 3. Analysis of Variance for SN ratios

Source	DF	Seq SS	Adj SS	Adj MS	F	P
Texture Type	3	28.11	29.02	9.67	0,03	0,992
Scanned Factor	3	512.04	720.04	240,01	0,76	0,571
Laser Power	3	1133.41	1133.41	377,81	1,20	0,417
Residual Error	4	1259.14	1259.14	314,79		
Total	13	2932.70				

From the main effect plots, a relationship between experiment parameters and contact angle can be seen in the main effect plots, as seen from Figure 5. According to Figure 5-a, the highest contact angles were obtained when the circle was the texture type. When diamond was the texture type, the most hydrophilic surfaces were obtained. It is noticed that by increasing the scanned factor, hydrophobicity increases. Increasing the laser power provides an increase and a zigzag-shaped decrease for the contact angle.

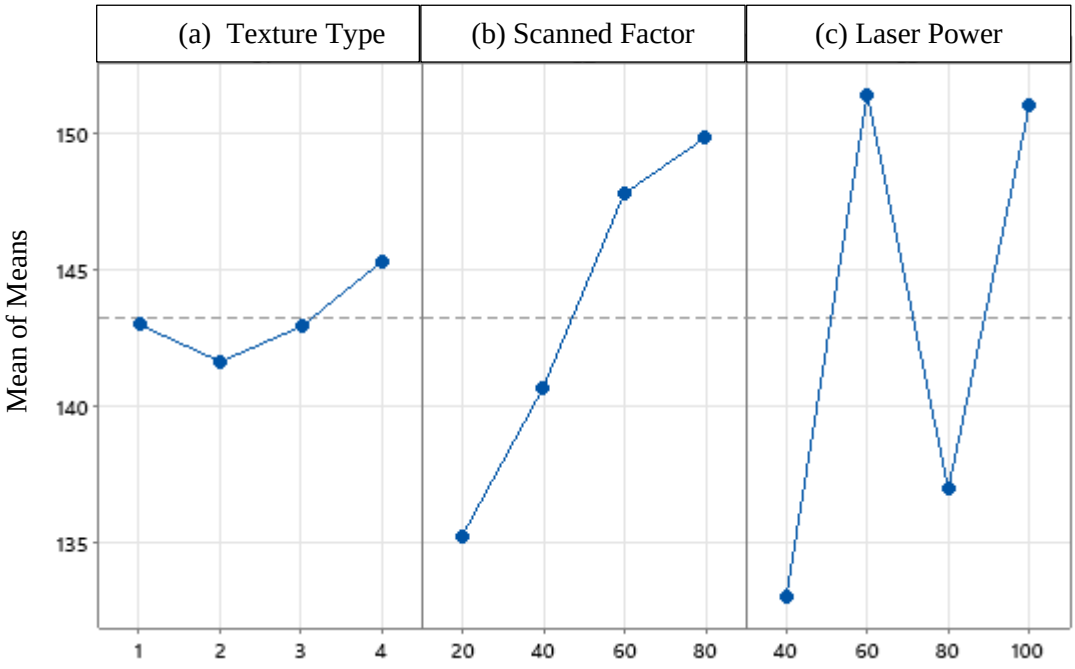

Figure 5. *Mean Effect Plots for contact angle*

3.4. Linear Regression Equations

A linear regression equation is a mathematical model that explains the relationship between a dependent variable and one or more independent variables by drawing a straight line through data points. Linear regression is a widely used engineering technique for system optimization and predictive modelling. Such regression analysis in process engineering, materials science, and quality control helps engineers analyze the relationship of variables. The uses it can put into practice include estimation of thermal characteristics in heat transfer systems, the optimization of manufacturing processes in determining factors affecting production efficiency, and the forecasting of mechanical parts' wear in time. Linear regression will also work to define the correlations of input parameters with outputs, which, in turn, can enable the engineer to make informed decisions, optimize designs, and improve dependability and performance.

$$For\ square: Contact\ angle = 116.0 + 0.267 \times (SF) + 0.194 \times (LP)$$

$$For\ diamond: Contact\ angle = 114.7 + 0.267 \times (SF) + 0.194 \times (LP)$$

$$For\ Hexagon: Contact\ angle = 116.0 + 0.267 \times (SF) + 0.194 \times (LP)$$

$$For\ Circle: Contact\ angle = 118.4 + 0.267 \times (SF) + 0.194 \times (LP)$$

Where SF is the theoretical laser scanned area factor, LP is the laser power.

4. Conclusions

The current study comprehensively investigates the LST of AA1050 aluminum alloy, focusing on the optimization of geometric patterns and laser parameters such as laser power and theoretical scanned area factor. The objective was to enhance two critical properties: surface roughness and wettability, which are of high importance when industrial applications require modified surface characteristics.

The results show that, among others, laser power is the most influential parameter on both surface roughness and hydrophobicity, contributing 64.97% according to ANOVA analysis. It can then be noticed that the increase in laser power makes the surface smoother, hence a decrease in surface roughness, while low power input and high factors of scanning area result in increased texturing, hence a high roughness of the surface. The pattern shapes tested included square, diamond, hexagon, and circle; the highest contact angle obtained with respect to the most hydrophobic surface for the conditions of laser power corresponded to the circular pattern. The least important factor for any of the tested geometric patterns was only 0.49% of the overall effect.

Regarding Sa values referring to surface roughness, it was observed that with lower laser power and scanning area factors increased, it produced more pronounced coarser textures, whereas at higher power, it smoothed the surface. For example, for square patterns processed at 40 W and an 80% scanned area factor, the highest roughness was recorded, whereas increasing it to a power of 100 W and with a smaller area factor, the surface flattened, which decreased clarity in the texture.

Funding Information

This work was supported by the Kocaeli University Scientific Research Projects Coordination Unit [Project No: FBA-2024-3704].

References

[1] Eneko Sáenz de Argandoña, Alaitz Zabala, Lander Galdos, Joseba Mendiguren, The Effect of Material Surface Roughness in Aluminum Forming, Procedia Manufacturing, Volume 47, 2020, Pages 591-595, ISSN 2351-9789, https://doi.org/10.1016/j.promfg.2020.04.182.

[2] Olatz Adarraga, Cecilia Agustín-Sáenz, Izaskun Bustero Fabiola Brusciotti, Superhydrophobic and oleophobic microtextured aluminum surface with long durability under corrosive environment. Sci Rep 13, 1737 (2023). https://doi.org/10.1038/s41598-023-28587-z

[3] Ahuir-Torres, J.I.; Kotadia, H.R.; Öpoz, T.T.; Sharp, M.C. A Study on the Corrosion Behaviour of Laser Textured Pure Aluminium in Saltwater. Processes 2023, 11, 721. https://doi.org/10.3390/pr11030721

[4] Ludmila B. Boinovich, Alexandre M. Emelyanenko, Alexander D. Modestov, Alexandr G. Domantovsky, and Kirill A. Emelyanenko, Synergistic Effect of Superhydrophobicity and Oxidized Layers on Corrosion Resistance of Aluminum Alloy Surface Textured by Nanosecond Laser Treatment, ACS Applied Materials & Interfaces 2015 7 (34), 19500-19508, DOI: 10.1021/acsami.5b06217

[5] Ali Heidarinejad, Fakhreddin Ashrafizadeh, Influence of surface texture and coating thickness on adhesion of nickel plated coatings to aluminium substrate, Journal of Manufacturing Processes, Volume 120, 2024, Pages 435-448, ISSN 1526-6125, https://doi.org/10.1016/j.jmapro.2024.04.040.

[6] Wojciech J. Stępniowski, Tomasz Durejko, Marta Michalska-Domańska, Magdalena Łazińska, Justyna Aniszewska, Characterization of nanoporous anodic aluminum oxide formed on laser pre-treated aluminum, Materials Characterization, Volume 122, 2016, Pages 130-136, ISSN 1044-5803, https://doi.org/10.1016/j.matchar.2016.10.034.

[7] Junying Min, Hailang Wan, Blair E. Carlson, Jianping Lin, Chengcheng Sun, Application of laser ablation in adhesive bonding of metallic materials: A review, Optics & Laser Technology, Volume 128, 2020, 106188, ISSN 0030-3992, https://doi.org/10.1016/j.optlastec.2020.106188.

[8] D. Bergström, J. Powell, and A. F. H. Kaplan, "Absorptance of nonferrous alloys to Nd:YLF and Nd:YAG laser light at room temperature," Appl. Opt. 46, 1290-1301 (2007), https://doi.org/10.1364/AO.46.001290

[9] Anas Ahmad Siddiqui, Avanish Kumar Dubey, Christ Prakash Paul, A study of metallurgy and erosion in laser surface alloying of AlxCu0.5FeNiTi high entropy alloy, Surface and Coatings Technology, Volume 361, 2019, Pages 27-34, ISSN 0257-8972, https://doi.org/10.1016/j.surfcoat.2019.01.042.